

# The complete-experiment problem of photoproduction of pseudoscalar mesons in a truncated partial-wave analysis

Y. Wunderlich,<sup>1</sup> R. Beck,<sup>1</sup> and L. Tiator<sup>2</sup>

<sup>1</sup>*Helmholtz-Institut für Strahlen- und Kernphysik, Universität Bonn, Bonn, Germany*

<sup>2</sup>*Institut für Kernphysik, Johannes Gutenberg-Universität Mainz, Mainz, Germany*

(Received 2 December 2013; published 12 May 2014)

The complete-experiment problem in the truncated partial-wave analysis (PWA) of pseudoscalar meson photoproduction with suppressed  $t$ -channel exchanges is investigated. The focus is set to ambiguities of the group S observables with the unpolarized differential cross section,  $\sigma_0$ , and the three single-spin observables,  $\Sigma$ ,  $T$ , and  $P$ . For this purpose, the approach and formalism already worked out by Omelaenko [Sov. J. Nucl. Phys. **34**, 406 (1981)] is revisited in this work. A numerical study using multipoles of the PWA solution MAID2007 shows how only one additional double polarization observable can resolve all ambiguities. Therefore, the possibility emerges to perform a complete experiment with only five observables.

DOI: [10.1103/PhysRevC.89.055203](https://doi.org/10.1103/PhysRevC.89.055203)

PACS number(s): 11.80.Et, 13.60.Le, 25.20.Lj

## I. INTRODUCTION

The nucleon and its excitation spectrum is of fundamental interest for our understanding of the visible nature in terms of quantum chromodynamics (QCD) in the nonperturbative regime. Whereas the nucleon itself is mainly investigated in electron scattering by its form factors and densities as well as in Compton scattering by polarizabilities, the excitation spectrum is traditionally explored in elastic and inelastic pion nucleon scattering and meson photo- and electroproduction. While the electromagnetic excitation of nucleon resonances was for a long time just the source for obtaining the photon decay amplitudes and the transition form factors, in recent years, the accuracy of data in photo- and electroproduction has increased so much that this reaction has now also become a source for possible observations of new resonances or for confirmations and establishments of such resonances that have only been “seen” in other reactions with rather uncertain parameters in the Particle Data Listings. Just recently, in the 2012 issue of the listings of the Particle Data Group (PDG), a series of  $N^*$  resonances has been established mainly owing to precise data in kaon photoproduction [1,2].

The simplest process to detect and to study nucleon resonances is the elastic pion nucleon scattering. It has the largest cross sections, it is a two-body process with a simple kinematical structure, and it is described by only two spin degrees of freedom, giving rise to two scattering amplitudes and four polarization observables. This field was pioneered by Hoehler [3] and Cutkosky *et al.* [4] and led to the detection of most of the  $N^*$  and  $\Delta$  resonances. Their determinations of masses, widths, partial decay widths, pole positions, and residues are still considered to be of high quality in the PDG. After the shutdown of the pion beams, experimental activities in pion nucleon scattering practically stopped about 20 yr ago. Nevertheless, impressive progress has been achieved in the past decade, mostly by improving the analyzing tools and developments of various models, primarily the dynamical models, some of them with eight and more coupled channels [5–11].

However, the construction of modern electron accelerators, new detector systems, and polarized targets led to enormous

progress in experiments in photo- and electroproduction. Next to pion nucleon scattering, the photoproduction of pseudoscalar mesons ( $\pi, \eta, \eta', K$ ) is the simplest process to analyze. It is described by four spin degrees of freedom with four complex amplitudes, usually given as CGLN (Chew, Goldberger, Low, and Nambu [12]), invariant, helicity, or transversity amplitudes, all of them linearly related to each other. With these four amplitudes, 16 polarization observables are defined and can be measured with linearly or circularly polarized photon beams, polarized targets, and recoil polarization detection.

Already around the year 1970 people started to think about how to determine the four complex helicity amplitudes for pseudoscalar meson photoproduction from a complete set of experiments. In 1975 Barker, Donnachie, and Storrow published their classical paper on “Complete Experiments” [13]. After reconsiderations and careful studies of discrete ambiguities, in the 1990s [14,15] it became clear that such a model-independent amplitude analysis would require at least eight polarization observables (including the unpolarized cross section), which have to be carefully chosen. There are a large number of possible combinations, but all of them would require a polarized beam and target and, in addition, recoil polarization measurements. Technically this was not possible until very recently, when transversely polarized targets came into operation at Mainz, Bonn, and JLab and, furthermore, recoil polarization measurements by nucleon rescattering have been shown to be doable.

A complete experiment is a set of measurements that is sufficient to predict all other possible experiments, provided that the measurements are free of uncertainties. Therefore, it is first of all an academic problem, which can be solved by mathematical algorithms. In practice, however, it will not work in the same way and either a very high statistical precision would be required, which is very unlikely, or further measurements of other polarization observables are necessary. This has been studied by Ireland [16] with information entropy, by a joint Mainz/GWU collaboration [17] with event-based pseudodata generated from the MAID model [6], by a JLab collaboration with both experimental and pseudodata for kaon

photoproduction [18] and in a very recent work by the Ghent group [19] with a combination of kaon photoproduction data measured at GRAAL and additional pseudodata from a theoretical model. In fact, photoproduction of  $K\Lambda$  and  $K\Sigma$  are ideal for the complete-experiment analysis, as the necessary recoil polarization observables can be obtained from the self-analyzing decay of the hyperons. In case of pion and  $\eta$  photoproduction this is very different and recoil polarization can only be detected by an additional elastic scattering of the outgoing nucleon on a spin-zero nucleus as  $^{12}\text{C}$  [20]. This reduces already very much the count rates, but even more, it does only allow a measurement of the transverse component of the recoil polarization in the laboratory frame. In this way, the necessary recoil polarization observables in the center-of-mass-system (CMS) frame cannot be measured.

However, even for kaon photoproduction, where the first complete-experiment analysis is only a question of time, an important problem remains with the unknown overall phase. Any set of quadratic equations must suffer from the problem that the underlying amplitudes can only be solved up to an overall phase. For the four complex amplitudes in pseudoscalar photoproduction, this means that the full solution gives just four absolute magnitudes and three relative phases. The residual overall phase remains undetermined. In the literature, two methods have been discussed, which are both highly academic and cannot be used in practice. The first goes back to Goldberger [21] in 1963 with a Hanbury-Brown and Twiss experiment; the second was recently published by Ivanov [22] in 2012, using vortex beams to measure the phase of a scattering amplitude. Even though the missing overall phase is no problem for reconstructing all 16 possible polarization observables, it does not make it possible to perform a partial-wave expansion, because this phase is a function of both energy and angle [23,24]. Nevertheless, if the complete experiment can be performed, it will be the optimal condition for a partial-wave analysis.

To obtain the partial-wave amplitudes and subsequently the information on nucleon resonances, another approach has to be undertaken, the truncated partial-wave analysis (TPWA). In this method, all 16 polarization observables are expanded in a partial-wave series up to a given maximal angular momentum  $\ell_{\max}$ , where all partial-wave amplitudes are only functions of the energy. In 1981 Omelaenko [25] showed that such a complete TPWA is possible with even less than eight observables. In fact, he proved that with only four observables—unpolarized cross section  $\sigma_0$ , photon beam asymmetry  $\Sigma$ , target polarization  $T$ , and recoil polarization  $P$ —the sets of quadratic equations with multipoles can be solved up to a discrete ambiguity for any given  $\ell_{\max}$ . To resolve this final ambiguity, only one more double polarization is needed, e.g.,  $F, G, C_{x'}, O_{x'}, C_{z'}, O_{z'}$ , while a measurement of  $E$  or  $H$  would not suffice. This is a rather surprising result, as it even allows a complete analysis for pion or  $\eta$  photoproduction without the need of recoil polarization observables. The single recoil polarization  $P$  can more easily be measured in a beam-target double polarization experiment.

As in the previous case, the full solution will determine all partial waves only up to an overall phase; however, this phase is now only dependent on the energy, and with some

theoretical assumptions, e.g., unitarity and Watson theorem, this phase can be constructed. This was first performed for  $\ell_{\max} = 1$  in 1989 by Grushin *et al.* [26] for a complete TPWA in the  $\Delta$  region.

The aim of this paper is to revisit the Omelaenko paper [25], published more than 30 yr ago. The formalism of this paper is not so easy to follow in the shortness of the original publication and the paper never gained much attention. We have extended and further clarified the formalism and have applied the method of ambiguities to modern partial-wave analyses (PWAs) as MAID [27], SAID [28], and BnGa [29]. Furthermore, we have also considered truncations beyond  $S + P$  waves and discuss also higher partial waves. We also investigate the possibilities for unique numerical solutions with current PWAs.

The work of Omelaenko is based on investigations on ambiguities arising in the analysis of  $\pi N$  scattering that were performed by Gersten [30] in 1969. Both approaches proceed via appropriately representing the spin amplitudes describing the process by products. For the sake of completeness, it should also be mentioned that for  $\pi N$  scattering an alternative scheme for obtaining product representations was proposed by Barrelet [31] in 1972 (see Ref. [32] for a brief treatment on this subject). The latter approach is generally referred to as the method of Barrelet zeros.

After a general introduction to the basics of the pseudoscalar meson photoproduction process, in Sec. III we derive the ambiguities of the group S observables (unpolarized cross section  $\sigma_0$ , photon beam asymmetry  $\Sigma$ , target asymmetry  $T$ , and nucleon recoil polarization  $P$ ) for reconstructing e.m. multipoles following the method of Omelaenko. In Sec. IV we discuss the behavior of double polarization observables and their ability to resolve ambiguities in the partial-wave solutions. In Sec. V we present a detailed study of the example with  $\ell_{\max} = 1$ . At the end we give a short summary and an outlook for applications with experimental data in the near future. In the appendixes we finally collect somewhat lengthy but useful mathematical formalism.

## II. BASIC DEFINITIONS

For photoproduction of pseudoscalar mesons on the nucleon,

$$\gamma N \rightarrow \varphi B, \quad (1)$$

where  $\varphi$  denotes the pseudoscalar meson and  $B$  the recoil baryon in the final state, the amplitude can be written in a general form [12],

$$\mathcal{F} = \chi_{m_{s_i}}^\dagger F_{\text{CGLN}} \chi_{m_{s_f}}. \quad (2)$$

The spinors  $\chi_{m_{s_i}}$  and  $\chi_{m_{s_f}}$  describe the initial nucleon as well as the recoil baryon in the final state. The spin operator  $F_{\text{CGLN}}$  appearing in Eq. (2) has the following expansion into spin momentum terms [12]:

$$F_{\text{CGLN}} = i\vec{\sigma} \cdot \hat{\epsilon} F_1 + \vec{\sigma} \cdot \hat{q} \vec{\sigma} \cdot \hat{k} \times \hat{\epsilon} F_2 + i\vec{\sigma} \cdot \hat{k} \hat{q} \cdot \hat{\epsilon} F_3 + i\vec{\sigma} \cdot \hat{q} \hat{q} \cdot \hat{\epsilon} F_4. \quad (3)$$

In Eq. (3),  $\hat{\epsilon}$  denotes the polarization unit vector of the incoming photon and  $\hat{k} = \vec{k}/|\vec{k}|$  as well as  $\hat{q} = \vec{q}/|\vec{q}|$  are

the normalized 3-momenta of the incoming and outgoing particles in the CMS. The complex coefficients  $\{F_i(W, \theta), i = 1, \dots, 4\}$ , carrying dependencies on the total CMS energy  $W$  and the CMS scattering angle  $\theta$  are called CGLN amplitudes. Once they are known, the photoproduction process is described completely. The angular dependence of the  $F_i(W, \theta)$  is given in terms of the multipole expansion [12,18],

$$F_1(W, \theta) = \sum_{\ell=0}^{\infty} \{[\ell M_{\ell+}(W) + E_{\ell+}(W)]P'_{\ell+1}(\cos \theta) + [(\ell+1)M_{\ell-}(W) + E_{\ell-}(W)]P'_{\ell-1}(\cos \theta)\}, \quad (4)$$

$$F_2(W, \theta) = \sum_{\ell=1}^{\infty} [(\ell+1)M_{\ell+}(W) + \ell M_{\ell-}(W)]P'_{\ell}(\cos \theta), \quad (5)$$

$$F_3(W, \theta) = \sum_{\ell=1}^{\infty} \{[E_{\ell+}(W) - M_{\ell+}(W)]P''_{\ell+1}(\cos \theta) + [E_{\ell-}(W) + M_{\ell-}(W)]P''_{\ell-1}(\cos \theta)\}, \quad (6)$$

$$F_4(W, \theta) = \sum_{\ell=2}^{\infty} [M_{\ell+}(W) - E_{\ell+}(W) - M_{\ell-}(W) - E_{\ell-}(W)] \times P''_{\ell}(\cos \theta), \quad (7)$$

where the electric and magnetic multipoles  $E_{\ell\pm}$  and  $M_{\ell\pm}$  describe transitions induced by electric and magnetic photons, respectively. The summation index  $\ell$  quantizes the orbital angular momentum of the final  $\varphi B$  system, which has a total angular momentum  $J = \ell \pm 1/2$ , and  $P_{\ell}(\cos \theta)$  are the Legendre polynomials.

For certain photoproduction channels ( $\gamma p \rightarrow \pi^0 p$  is an important example but  $\gamma p \rightarrow \eta p$  is also applicable), close to production thresholds, and in the low-energy region, a truncation of the infinite series (4) to (7) at a finite value  $\ell_{\max} = L$  already yields a good approximation for the  $F_i$  [18]. Those channels are at the center of attention in this work. Besides the CGLN amplitudes  $F_i$ , also other sets of amplitudes, helicity, transversity, and invariant amplitudes are commonly used. The transversity amplitudes  $\{b_i(W, \theta), i = 1, \dots, 4\}$  are defined by a rotation of the spin quantization axis of the target nucleon and recoil baryon to the normal of the reaction plane [13,33],

$$b_1(W, \theta) = -b_3(W, \theta) + iC \sin \theta [F_3(W, \theta)e^{-i\frac{\theta}{2}} + F_4(W, \theta)e^{i\frac{\theta}{2}}], \quad (8)$$

$$b_2(W, \theta) = -b_4(W, \theta) - iC \sin \theta [F_3(W, \theta)e^{i\frac{\theta}{2}} + F_4(W, \theta)e^{-i\frac{\theta}{2}}], \quad (9)$$

$$b_3(W, \theta) = C[F_1(W, \theta)e^{-i\frac{\theta}{2}} - F_2(W, \theta)e^{i\frac{\theta}{2}}], \quad (10)$$

$$b_4(W, \theta) = C[F_1(W, \theta)e^{i\frac{\theta}{2}} - F_2(W, \theta)e^{-i\frac{\theta}{2}}]. \quad (11)$$

In the following, we drop the  $W$  dependence of the amplitudes and all further considerations and analyses will be single-energy analyses, where the energy  $W$  is kept fixed.  $C$  is a complex factor depending on the convention chosen for the definition of amplitudes. The value  $C = i/\sqrt{2}$  is consistent with this work. The convention for the definition of the  $b_i$

is consistent with Ref. [33]. Inspection of Eqs. (4) to (7), as well as the fact that the function  $\cos \theta$  is symmetric under the angular reflection  $\theta \rightarrow -\theta$ , leads to the following symmetry of the CGLN amplitudes

$$F_i(\theta) = F_i(-\theta), \quad i = 1, \dots, 4. \quad (12)$$

The combination of this symmetry property with the definitions of transversity amplitudes (8) to (11) deduces the following relations valid for the  $b_i$

$$b_1(\theta) = b_2(-\theta), \quad b_3(\theta) = b_4(-\theta). \quad (13)$$

It appears now that only two complex amplitudes are necessary to describe the photoproduction process. While the CGLN amplitudes are even functions in  $\theta$ , the transversity amplitudes do not have a definite symmetry and, as it is shown, by extending the functions to negative values, two of them give just redundant information. Therefore, in the following it is enough to consider just only two transversity functions  $b_2$  and  $b_4$ .

It should be noted that the equations relating transversity to CGLN amplitudes are linear, i.e.,

$$b_i = \sum_{j=1}^4 \hat{T}_{ij} F_j. \quad (14)$$

This means that once a particular system of spin amplitudes is known, the other one is as well.

For pseudoscalar meson photoproduction, there are, in principle, 16 measurable polarization observables. These observables group into the four classes of group S observables  $\{\sigma_0, \Sigma, T, P\}$  containing also the unpolarized cross section  $\sigma_0 = d\sigma/d\Omega$ , beam-target (BT) observables  $\{E, F, G, H\}$ , beam-recoil (BR) observables  $\{C_{x'}, C_{z'}, O_{x'}, O_{z'}\}$ , and target-recoil (TR) observables  $\{T_{x'}, T_{z'}, L_{x'}, L_{z'}\}$  [13,34].

Table I summarizes the definitions of observables used in this work. Because transversity amplitudes are used in the following discussion, the observables are tabulated exclusively

TABLE I. Polarization observables listed with sign choices that are consistent with the MAID PWA [13,27]; for other conventions, see Ref. [34]. Observables are written using transversity amplitudes.

| Observable                  | Transversity representation                           | Type |
|-----------------------------|---|------|
| $I(\theta) = \sigma_0/\rho$ | $\frac{1}{2}( b_1 ^2 +  b_2 ^2 +  b_3 ^2 +  b_4 ^2)$  | S    |
| $\check{\Sigma}$            | $\frac{1}{2}(- b_1 ^2 -  b_2 ^2 +  b_3 ^2 +  b_4 ^2)$ |      |
| $\check{T}$                 | $\frac{1}{2}( b_1 ^2 -  b_2 ^2 -  b_3 ^2 +  b_4 ^2)$  |      |
| $\check{P}$                 | $\frac{1}{2}(- b_1 ^2 +  b_2 ^2 -  b_3 ^2 +  b_4 ^2)$ |      |
| $\check{G}$                 | $\text{Im}[-b_1 b_3^* - b_2 b_4^*]$                   | BT   |
| $\check{H}$                 | $-\text{Re}[b_1 b_3^* - b_2 b_4^*]$                   |      |
| $\check{E}$                 | $-\text{Re}[b_1 b_3^* + b_2 b_4^*]$                   |      |
| $\check{F}$                 | $\text{Im}[b_1 b_3^* - b_2 b_4^*]$                    |      |
| $\check{O}_{x'}$            | $-\text{Re}[-b_1 b_4^* + b_2 b_3^*]$                  | BR   |
| $\check{O}_{z'}$            | $\text{Im}[-b_1 b_4^* - b_2 b_3^*]$                   |      |
| $\check{C}_{x'}$            | $\text{Im}[b_1 b_4^* - b_2 b_3^*]$                    |      |
| $\check{C}_{z'}$            | $\text{Re}[b_1 b_4^* + b_2 b_3^*]$                    |      |
| $\check{T}_{x'}$            | $-\text{Re}[-b_1 b_2^* + b_3 b_4^*]$                  | TR   |
| $\check{T}_{z'}$            | $-\text{Im}[b_1 b_2^* - b_3 b_4^*]$                   |      |
| $\check{L}_{x'}$            | $-\text{Im}[-b_1 b_2^* - b_3 b_4^*]$                  |      |
| $\check{L}_{z'}$            | $\text{Re}[-b_1 b_2^* - b_3 b_4^*]$                   |      |

in terms of the  $b_i$ . Independently of the system of spin amplitudes used, every observable  $\Omega$  is defined by a profile function  $\tilde{\Omega}$  that is a bilinear Hermitian form of the amplitudes. To obtain an observable from the corresponding profile function, the latter has to be divided by the unpolarized cross section. The conventions for observables used in this work are consistent with those of Refs. [13] and [27].

### III. FORMALISM FOR THE STUDY OF AMBIGUITIES OF THE GROUP S OBSERVABLES FOR A TPWA WITH $\ell \leq L$

This section presents an ambiguity study of the group S observables. The fundamental idea for this study, as presented in Refs. [25] and [30], consists of exchanging the angular variable  $\cos \theta$  present in the multipole expansion of Eqs. (4) to (7) for  $t = \tan \theta/2$ .

The fundamental trigonometric functions  $\sin \theta$  and  $\cos \theta$  expressed in terms of  $\tan \theta/2$  read [30]

$$\sin \theta = \frac{2 \tan \frac{\theta}{2}}{1 + \tan^2 \frac{\theta}{2}}, \quad \cos \theta = \frac{1 - \tan^2 \frac{\theta}{2}}{1 + \tan^2 \frac{\theta}{2}}. \quad (15)$$

The relation for  $\cos \theta$  can be formally inverted as follows:

$$\tan \frac{\theta}{2} = \begin{cases} +\sqrt{\frac{1-\cos \theta}{1+\cos \theta}}, & \theta \in [0, \pi], \\ -\sqrt{\frac{1-\cos \theta}{1+\cos \theta}}, & \theta \in [-\pi, 0]. \end{cases} \quad (16)$$

Therefore,  $\cos \theta$  and  $t = \tan \theta/2$  are recognized as fully equivalent angular variables. As shown in Ref. [25] and Appendix A, the multipole expansions of the transversity amplitudes  $b_2$  and  $b_4$  up to a finite truncation angular momentum  $L$  take the form

$$b_4(\theta) = C \frac{\exp(i\frac{\theta}{2})}{(1+t^2)^L} A'_{2L}(t), \quad (17)$$

$$b_2(\theta) = -C \frac{\exp(i\frac{\theta}{2})}{(1+t^2)^L} [A'_{2L}(t) + t D'_{2L-2}(t)], \quad (18)$$

when written in terms of  $t$ .  $A'_{2L}(t)$  and  $D'_{2L-2}(t)$  are polynomials in  $t$  with generally complex coefficients. The definition of  $B'_{2L}(t) = A'_{2L}(t) + t D'_{2L-2}(t)$  simplifies Eq. (18). Once the amplitudes  $b_2$  and  $b_4$  are known, the remaining functions  $b_1$  and  $b_3$  can be obtained from Eq. (13). This fact is used repeatedly in the remaining discussion. Appendix A contains a derivation of the expression for  $A'_{2L}(t)$  that reads

$$\begin{aligned} A'_{2L}(t) = & \frac{1}{2} \sum_{\ell=0}^L \{ f_{\ell}^{(1)}(\ell+1)(\ell+2)(1+t^2)^{L-\ell} {}_2F_1(-\ell, -\ell-1; 2; -t^2) \\ & + f_{\ell}^{(2)}\ell(\ell-1)(1+t^2)^{L-\ell+2} {}_2F_1(-\ell+2, -\ell+1; 2; -t^2) \\ & + f_{\ell}^{(3)}\ell(\ell+1)(t+i)^2(1+t^2)^{L-\ell} {}_2F_1(-\ell+1, -\ell; 2; -t^2) \}, \end{aligned} \quad (19)$$

containing hypergeometric functions  ${}_2F_1(a, b; c; Z)$  (see also [25] and [30]).

$B'_{2L}(t)$  composes by adding a similarly looking expansion, i.e.,  $D'_{2L-2}(t)$ ,

$$\begin{aligned} B'_{2L}(t) = & A'_{2L}(t) + \frac{t}{4} \sum_{\ell=0}^L \{ (i f_{\ell}^{(4)})\ell(\ell+1)(\ell+2)(\ell+3)(1+t^2)^{L-\ell} {}_2F_1(-\ell+1, -\ell-1; 3; -t^2) \\ & + (i f_{\ell}^{(5)})(\ell-2)(\ell-1)\ell(\ell+1)(1+t^2)^{L-\ell+2} {}_2F_1(-\ell+3, -\ell+1; 3; -t^2) \\ & - (i f_{\ell}^{(6)})(\ell-1)\ell(\ell+1)(\ell+2)(t+i)^2(1+t^2)^{L-\ell} {}_2F_1(-\ell+2, -\ell; 3; -t^2) \}, \end{aligned} \quad (20)$$

with the definitions of six partial-wave coefficients (see Appendix A):

$$f_{\ell}^{(1)} = \ell M_{\ell+} + E_{\ell+}, \quad (21)$$

$$f_{\ell}^{(2)} = (\ell+1)M_{\ell-} + E_{\ell-}, \quad (22)$$

$$f_{\ell}^{(3)} = (\ell+1)M_{\ell+} + \ell M_{\ell-}, \quad (23)$$

$$f_{\ell}^{(4)} = E_{\ell+} - M_{\ell+}, \quad (24)$$

$$f_{\ell}^{(5)} = E_{\ell-} + M_{\ell-}, \quad (25)$$

$$f_{\ell}^{(6)} = M_{\ell+} - E_{\ell+} - M_{\ell-} - E_{\ell-}. \quad (26)$$

Once the expressions (19) and (20) are evaluated for a specific  $L$ , both reduce to polynomials in the variable  $t$  having the finite

order  $2L$  and complex coefficients  $a_{\ell}, b_{\ell}$ ,

$$A'_{2L}(t) = \sum_{\ell=0}^{2L} a_{\ell} t^{\ell}, \quad (27)$$

$$B'_{2L}(t) = \sum_{\ell=0}^{2L} b_{\ell} t^{\ell}. \quad (28)$$

There appear  $4L+2$  expansion coefficients in Eqs. (27) and (28) that have to contain the same information content as the  $4L$  multipoles for a finite  $L$  [see Eqs. (4) to (7)]. This counting suggests that not all of the coefficients  $a_{\ell}$  and  $b_{\ell}$  are independent. This can be seen by first investigating Eq. (18) and noting that the polynomial  $D'_{2L-2}(t)$  only has order  $2L-2$ , which means that the leading coefficients of  $A'_{2L}(t)$  and  $B'_{2L}(t)$  are equal [see also (20)]. The term  $t D'_{2L-2}(t)$  is zero

for  $t = 0$  and for every order in  $L$ . Therefore, also the free terms of  $A'_{2L}(t)$  and  $B'_{2L}(t)$  are equal, i.e.,  $A'_{2L}(t = 0) \equiv B'_{2L}(t = 0)$ . Both facts are expressed in the relations

$$a_{2L} = b_{2L}, \quad a_0 = b_0. \quad (29)$$

A next convenient step is taken in Ref. [25] by defining normalized versions of  $A'_{2L}(t)$  and  $B'_{2L}(t)$  by

$$A'_{2L}(t) = a_{2L} A_{2L}(t), \quad (30)$$

$$B'_{2L}(t) = a_{2L} B_{2L}(t), \quad (31)$$

where the first identity  $a_{2L} = b_{2L}$  of Eq. (29) is already invoked. In terms of the normalized polynomials  $A_{2L}(t)$  and  $B_{2L}(t)$  the amplitudes  $b_2$  and  $b_4$  take the form

$$b_4(\theta) = C a_{2L} \frac{\exp(i\frac{\theta}{2})}{(1+t^2)^L} A_{2L}(t), \quad (32)$$

$$b_2(\theta) = -C a_{2L} \frac{\exp(i\frac{\theta}{2})}{(1+t^2)^L} B_{2L}(t), \quad (33)$$

and both normalized polynomials can be written as

$$A_{2L}(t) = t^{2L} + \sum_{\ell=0}^{2L-1} \hat{a}_\ell t^\ell, \quad (34)$$

$$B_{2L}(t) = t^{2L} + \sum_{\ell=0}^{2L-1} \hat{b}_\ell t^\ell, \quad (35)$$

with new coefficients  $\{\hat{a}_\ell = a_\ell/a_{2L} | \ell = 0, \dots, 2L-1\}$  and  $\{\hat{b}_\ell = b_\ell/b_{2L} | \ell = 0, \dots, 2L-1\}$ . The equality of the free terms also survives for the normalized polynomials, i.e.,

$$\hat{a}_0 = \hat{b}_0. \quad (36)$$

The number of independent complex coefficients in the present formulation consisting of  $a_{2L}$ ,  $\hat{a}_0$  and  $\{\hat{a}_\ell | \ell \neq 0\}$  and  $\{\hat{b}_\ell | \ell \neq 0\}$  counts as  $4L$  as it should. It is now crucial to note [25] that because  $A_{2L}(t)$  and  $B_{2L}(t)$  are complex polynomials, the fundamental theorem of algebra holds and both decompose into products of their linear factors as

$$A_{2L}(t) = \prod_{k=1}^{2L} (t - \alpha_k), \quad B_{2L}(t) = \prod_{k=1}^{2L} (t - \beta_k), \quad (37)$$

with  $\{\alpha_k \in \mathbb{C} | k = 1, \dots, 2L\}$  and  $\{\beta_k \in \mathbb{C} | k = 1, \dots, 2L\}$  the complex roots of  $A_{2L}(t)$  and  $B_{2L}(t)$ , respectively. In terms of a linear factorization (37), the transversity amplitudes  $b_4$  and  $b_2$  become

$$b_4(\theta) = C a_{2L} \frac{\exp(i\frac{\theta}{2})}{(1+t^2)^L} \prod_{k=1}^{2L} (t - \alpha_k), \quad (38)$$

$$b_2(\theta) = -C a_{2L} \frac{\exp(i\frac{\theta}{2})}{(1+t^2)^L} \prod_{k=1}^{2L} (t - \beta_k). \quad (39)$$

The equality of the free terms, i.e.,  $A_{2L}(t = 0) \equiv B_{2L}(t = 0)$ , yields [see Eq. (37)]

$$\prod_{k=1}^{2L} \alpha_k = \prod_{k=1}^{2L} \beta_k, \quad (40)$$

which will become an important relation in the following. Equation (40) is used to test if possible ambiguities of the group  $S$  observables are consistent with the underlying formalism. Therefore, it is named the consistency relation.

Another important object introduced in Ref. [25] is the root function  $f(\theta, \alpha)$  defined by

$$f(\theta, \alpha) = f(\theta, \alpha_1, \dots, \alpha_{2L}) = \frac{\prod_{k=1}^{2L} (\tan \frac{\theta}{2} - \alpha_k)}{(1 + \tan^2 \frac{\theta}{2})^L} \quad (41)$$

and  $f(\theta, \beta) = f(\theta, \beta_1, \dots, \beta_{2L})$ , accordingly. The following useful facts are valid for the root function:

$$f(\theta, \alpha)|_{\theta=0} = \prod_{k=1}^{2L} \alpha_k, \quad (42)$$

$$\lim_{\theta \rightarrow \pi} f(\theta, \alpha) = 1. \quad (43)$$

When expressed using the root function, the amplitudes  $b_4$  and  $b_2$  acquire the simple form

$$b_4(\theta) = C a_{2L} \exp\left(i\frac{\theta}{2}\right) f(\theta, \alpha), \quad (44)$$

$$b_2(\theta) = -C a_{2L} \exp\left(i\frac{\theta}{2}\right) f(\theta, \beta). \quad (45)$$

To obtain expressions for the remaining amplitudes  $b_3$  and  $b_1$ , the angular reflection  $\theta \rightarrow -\theta$ , as well as Eq. (13), have to be invoked. Under reflection, the root functions behave as

$$\begin{aligned} f(-\theta, \alpha) &= \frac{\prod_{k=1}^{2L} [\tan(-\frac{\theta}{2}) - \alpha_k]}{[1 + \tan^2(-\frac{\theta}{2})]^L} \\ &= \frac{\prod_{k=1}^{2L} (-\tan \frac{\theta}{2} - \alpha_k)}{[1 + (-\tan \frac{\theta}{2})^2]^L} \\ &= (-)^{2L} \frac{\prod_{k=1}^{2L} (\tan \frac{\theta}{2} + \alpha_k)}{(1 + \tan^2 \frac{\theta}{2})^L} \\ &= f(\theta, -\alpha). \end{aligned} \quad (46)$$

Therefore, the remaining transversity amplitudes can also be written in compact form as

$$b_3(\theta) = b_4(-\theta) = C a_{2L} \exp\left(-i\frac{\theta}{2}\right) f(\theta, -\alpha), \quad (47)$$

$$b_1(\theta) = b_2(-\theta) = -C a_{2L} \exp\left(-i\frac{\theta}{2}\right) f(\theta, -\beta). \quad (48)$$

For the remaining discussion, it is important to consider the behavior of the root functions under simultaneous complex conjugation of all roots  $\alpha \rightarrow \alpha^*$  or  $\beta \rightarrow \beta^*$ :

$$\begin{aligned} f(\theta, \alpha^*) &= \frac{\prod_{k=1}^{2L} (\tan \frac{\theta}{2} - \alpha_k^*)}{(1 + \tan^2 \frac{\theta}{2})^L} = \frac{\prod_{k=1}^{2L} (\tan \frac{\theta}{2} - \alpha_k)^*}{[(1 + \tan^2 \frac{\theta}{2})^*]^L} \\ &= \left[ \frac{\prod_{k=1}^{2L} (\tan \frac{\theta}{2} - \alpha_k)}{(1 + \tan^2 \frac{\theta}{2})^L} \right]^* \\ &= f^*(\theta, \alpha). \end{aligned} \quad (49)$$

Preceding the discussion of the ambiguity study of group S observables, it is reasonable to compare the number of independent real parameters in an ordinary TPWA and the reformulated version. In an energy-independent fit, the number of independent real parameters for every order in  $L$  counts as

$$8L - 1, \quad (50)$$

i.e.,  $4L$  complex multipoles with an undetermined overall phase. There should be an equal number of parameters in the reformulated version of the problem. The counting of the real degrees of freedom represented by the roots  $\{\alpha_k\}$  and  $\{\beta_k\}$  gives  $8L$ . Equation (40), reformulated as

$$\prod_{k=1}^{2L} \alpha_k \Big/ \prod_{k'=1}^{2L-1} \beta_{k'} = \beta_{2L}, \quad (51)$$

reduces the number of independent real degrees of freedom of the roots to  $8L - 2$ . There is one additional unknown complex variable in the reformulation,  $a_{2L}$ . The modulus  $|a_{2L}|$  can be determined from the forward-scattering cross section  $I(\pi)$  (see discussion below). The phase  $\phi_{2L}$  of  $a_{2L} = |a_{2L}|e^{i\phi_{2L}}$  cannot be obtained by multipole analysis. This leaves the anticipated number of  $8L - 1$  independent real parameters for the reformulation of the multipole expansion.

What remains to be done before the ambiguities of the group S observables are discussed is to establish a connection among the complex coefficient  $a_{2L}$  and the forward-scattering cross section  $I(\pi)$ . Utilizing the symmetry relation (13), the observable  $I(\theta)$  takes the form (see Table I)

$$I(\theta) = \frac{1}{2}[|b_2(-\theta)|^2 + |b_2(\theta)|^2 + |b_4(-\theta)|^2 + |b_4(\theta)|^2]. \quad (52)$$

In the limit  $\theta \rightarrow \pi$ , all root functions are unity [see Eq. (43)]. Therefore,

$$I(\theta)|_{\theta \rightarrow \pi} = I(\pi) = 2|\mathcal{C}|^2|a_{2L}|^2. \quad (53)$$

In this work, the consistent value for  $\mathcal{C}$  is  $i/\sqrt{2}$  and Eq. (53) yields  $I(\pi) = |a_{2L}|^2$ . This is the anticipated relation connecting the modulus  $|a_{2L}|$  to the unpolarized cross section for forward scattering.

With everything assembled until now, the possible ambiguities of multipole solutions for the group S observables can be discussed. Once the transversity amplitudes written in root functions [i.e., Eqs. (44), (45), (47), and (48)] are inserted into the group S observables of Table I, the latter take the form

$$I(\theta) = \frac{I(\pi)}{4}[|f(\theta, -\beta)|^2 + |f(\theta, \beta)|^2 + |f(\theta, -\alpha)|^2 + |f(\theta, \alpha)|^2], \quad (54)$$

$$\check{\Sigma}(\theta) = \frac{I(\pi)}{4}[-|f(\theta, -\beta)|^2 - |f(\theta, \beta)|^2 + |f(\theta, -\alpha)|^2 + |f(\theta, \alpha)|^2], \quad (55)$$

$$\check{T}(\theta) = \frac{I(\pi)}{4}[|f(\theta, -\beta)|^2 - |f(\theta, \beta)|^2 - |f(\theta, -\alpha)|^2 + |f(\theta, \alpha)|^2], \quad (56)$$

$$\check{P}(\theta) = \frac{I(\pi)}{4}[-|f(\theta, -\beta)|^2 + |f(\theta, \beta)|^2 - |f(\theta, -\alpha)|^2 + |f(\theta, \alpha)|^2]. \quad (57)$$

It can now be seen by inspection of the rule (49) that the group S observables as written above are invariant under the replacement

$$\alpha \rightarrow \alpha^*, \quad \beta \rightarrow \beta^*, \quad (58)$$

or, in more detail,

$$\alpha_i \rightarrow \alpha_i^*, \quad \beta_j \rightarrow \beta_j^*, \quad i, j = 1, \dots, 2L. \quad (59)$$

In Ref. [25], this replacement rule was named the double ambiguity. Once the newly obtained roots are resolved for the multipoles, the new solution will generally be distinct from the original one, but yield the same group S observables. Also, the new solutions obtained via the double ambiguity transformation automatically fulfill the consistency relation (40). Complex conjugation of both sides of Eq. (40) yields

$$\prod_{k=1}^{2L} \alpha_k^* = \prod_{k=1}^{2L} \beta_k^*, \quad (60)$$

which proves the latter claim.

However, the double ambiguity is not the only possible ambiguity of the group S observables, but every replacement similar to Eq. (59) with arbitrary subsets of indices  $\{i, j\}$  conjugated and all remaining indices not conjugated leaves the group S observables invariant. The only possibility to rule out those extra ambiguities is to check whether or not they fulfill the consistency relation (40). This fulfillment then would correspond to a numerical accident and cannot be predicted. The complex roots expressed in terms of phases read

$$\alpha_k = |\alpha_k|e^{i\varphi_k}, \quad \beta_k = |\beta_k|e^{i\psi_k}. \quad (61)$$

Using the quantities  $\varphi_k$  and  $\psi_k$ , the fact that an arbitrary combination of complex conjugations of the roots fulfills the consistency relation (40) is equivalent to the validity of the equation

$$\pm\varphi_1 \pm \dots \pm \varphi_{2L} = \pm\psi_1 \pm \dots \pm \psi_{2L}, \quad (62)$$

for an arbitrary choice of sign combinations. The number of candidates of additional solutions that can be formed by complex conjugation of the roots  $\{\alpha_k\}$  and  $\{\beta_k\}$ , because  $2^{2L}$  additional sets of  $\{\alpha_k\}$  and  $2^{2L}$  sets of  $\{\beta_k\}$  are possible, is  $4^{2L}$ . Therefore, the number of  $4^{2L}$  new potentially ambiguous solutions has to be tested whether or not they fulfill the consistency relation (40).

The sets of objects and formulas introduced until now facilitate an ambiguity study of the group S observables. This procedure consists of first beginning using a specific starting solution for multipoles (for example, taken from a PWA program) and then computing the roots  $\alpha$  and  $\beta$ . Once the roots are calculated, additional sets of solutions are obtained by complex conjugation, leaving the group S observables invariant. Next, for all of these additional solutions, including the double ambiguity, the behavior of the double polarization observables of the groups BT, BR, and TR under these new solutions has to be investigated. This investigation should then yield a set of double polarization observables that can remove all of the remaining ambiguities.

#### IV. BEHAVIOR OF DOUBLE POLARIZATION OBSERVABLES

First, the behavior of the BT observables shall be investigated. Inserting the transversity amplitude form of Eqs. (44), (45), (47), and (48) into the definitions (Table I) yields the expressions

$$\check{E}(\theta) = -\frac{I(\pi)}{2} \text{Re}[-f(\theta, -\beta)f^*(\theta, -\alpha) - f(\theta, \beta)f^*(\theta, \alpha)], \quad (63)$$

$$\check{F}(\theta) = \frac{I(\pi)}{2} \text{Im}[-f(\theta, -\beta)f^*(\theta, -\alpha) + f(\theta, \beta)f^*(\theta, \alpha)], \quad (64)$$

$$\check{G}(\theta) = \frac{I(\pi)}{2} \text{Im}[f(\theta, -\beta)f^*(\theta, -\alpha) + f(\theta, \beta)f^*(\theta, \alpha)], \quad (65)$$

$$\check{H}(\theta) = -\frac{I(\pi)}{2} \text{Re}[-f(\theta, -\beta)f^*(\theta, -\alpha) + f(\theta, \beta)f^*(\theta, \alpha)]. \quad (66)$$

TABLE II. Angular boundary values of all double polarization observables.

|                          | $E$ | $F$ | $G$ | $H$ | $C_{x'}$ | $C_{z'}$ | $O_{x'}$ | $O_{z'}$ | $T_{x'}$ | $T_{z'}$ | $L_{x'}$ | $L_{z'}$ |
|--------------------------|-----|-----|-----|-----|----------|----------|----------|----------|----------|----------|----------|----------|
| $\theta = 0$             | 1   | 0   | 0   | 0   | 0        | +1       | 0        | 0        | 0        | 0        | 0        | -1       |
| $\theta \rightarrow \pi$ | 1   | 0   | 0   | 0   | 0        | -1       | 0        | 0        | 0        | 0        | 0        | +1       |

First of all, it is important to note that the response of the BT observables to the double ambiguity transformation (58) can be predicted. Consulting the rule (49) describing the transformation of the root functions under the double ambiguity, it is evident that the observables  $\check{F}$  as well as  $\check{G}$ , whose definition involves the imaginary part, change sign in Eqs. (64) and (65). The observables defined via real parts, i.e.,  $\check{E}$  and  $\check{H}$ , are invariant under the double ambiguity. Therefore, they cannot resolve it. For the angular boundary values  $\theta = 0$  and  $\pi$  the root functions behave as  $f(\theta, \alpha)|_{\theta=0} = \prod_k \alpha_k$  and  $f(\theta, \alpha)|_{\theta \rightarrow \pi} = 1$ . Therefore, consulting Eqs. (63) to (66), the values taken by the BT observables on the angular boundaries can be summarized, as is done in Table II.

Second, the BR observables (Table I) expressed by the root function  $f$  read

$$\check{C}_{x'}(\theta) = \frac{I(\pi)}{2} \{\cos \theta \text{Im}[f(\theta, -\beta)f^*(\theta, \alpha) - f(\theta, \beta)f^*(\theta, -\alpha)] + \sin \theta \text{Re}[-f(\theta, \beta)f^*(\theta, -\alpha) - f(\theta, -\beta)f^*(\theta, \alpha)]\}, \quad (67)$$

$$\check{C}_{z'}(\theta) = \frac{I(\pi)}{2} \{\cos \theta \text{Re}[f(\theta, -\beta)f^*(\theta, \alpha) + f(\theta, \beta)f^*(\theta, -\alpha)] + \sin \theta \text{Im}[f(\theta, -\beta)f^*(\theta, \alpha) - f(\theta, \beta)f^*(\theta, -\alpha)]\}, \quad (68)$$

$$\check{O}_{x'}(\theta) = -\frac{I(\pi)}{2} \{\cos \theta \text{Re}[f(\theta, -\beta)f^*(\theta, \alpha) - f(\theta, \beta)f^*(\theta, -\alpha)] + \sin \theta \text{Im}[f(\theta, -\beta)f^*(\theta, \alpha) + f(\theta, \beta)f^*(\theta, -\alpha)]\}, \quad (69)$$

$$\check{O}_{z'}(\theta) = -\frac{I(\pi)}{2} \{\cos \theta \text{Im}[f(\theta, -\beta)f^*(\theta, \alpha) + f(\theta, \beta)f^*(\theta, -\alpha)] + \sin \theta \text{Re}[f(\theta, \beta)f^*(\theta, -\alpha) - f(\theta, -\beta)f^*(\theta, \alpha)]\}. \quad (70)$$

Because all of them involve terms with real and imaginary parts, they all change under the complex conjugation and, therefore, they all can resolve the double ambiguity. Furthermore, the values of the observables on the angular boundaries can be predicted. They are listed in Table II.

Finally, the TR observables (Table I) are also expressed in terms of the root function

$$\check{T}_{x'}(\theta) = -\frac{I(\pi)}{2} \{\cos \theta \text{Re}[f(\theta, -\beta)f^*(\theta, \beta) - f(\theta, -\alpha)f^*(\theta, \alpha)] + \sin \theta \text{Im}[f(\theta, -\beta)f^*(\theta, \beta) - f(\theta, -\alpha)f^*(\theta, \alpha)]\}, \quad (71)$$

$$\check{T}_{z'}(\theta) = \frac{I(\pi)}{2} \{\cos \theta \text{Im}[f(\theta, -\beta)f^*(\theta, \beta) - f(\theta, -\alpha)f^*(\theta, \alpha)] + \sin \theta \text{Re}[-f(\theta, -\beta)f^*(\theta, \beta) + f(\theta, -\alpha)f^*(\theta, \alpha)]\}, \quad (72)$$

$$\check{L}_{x'}(\theta) = \frac{I(\pi)}{2} \{\cos \theta \text{Im}[f(\theta, -\beta)f^*(\theta, \beta) + f(\theta, -\alpha)f^*(\theta, \alpha)] + \sin \theta \text{Re}[-f(\theta, -\beta)f^*(\theta, \beta) - f(\theta, -\alpha)f^*(\theta, \alpha)]\}, \quad (73)$$

$$\check{L}_{z'}(\theta) = \frac{I(\pi)}{2} \{\cos \theta \text{Re}[-f(\theta, -\beta)f^*(\theta, \beta) - f(\theta, -\alpha)f^*(\theta, \alpha)] + \sin \theta \text{Im}[-f(\theta, -\beta)f^*(\theta, \beta) - f(\theta, -\alpha)f^*(\theta, \alpha)]\}. \quad (74)$$

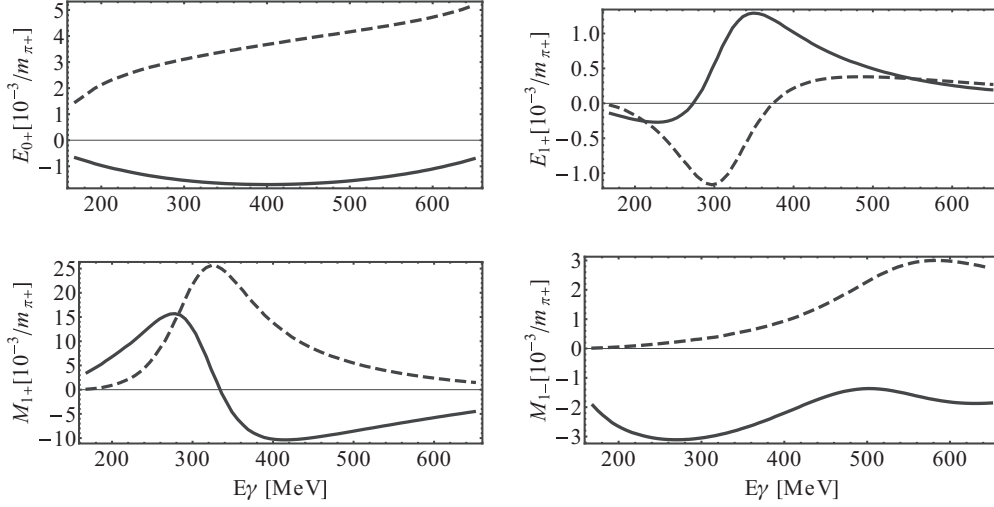


FIG. 1. Real (solid curves) and imaginary (dashed curves) parts of the  $S$ - and  $P$ -wave multipoles of the MAID2007 solution. All quantities are plotted versus the photon laboratory energy  $E_\gamma^{\text{LAB}}$ .

Again, all of them change under the complex conjugation and are able to resolve the double ambiguity. On the angular boundaries  $\theta = 0$  and  $\pi$  they take the values given in Table II.

### V. A COMPARATIVE NUMERICAL STUDY FOR $L = 1$

This section contains the depiction of a numerical ambiguity study performed using the formalism of Sec. III (see Ref. [25] for a similar study). The case  $L = 1$  is considered. As input for the study, multipoles are needed. The set of multipoles used in this case originates from the MAID solution MAID2007 (see Ref. [27]), more precisely the channel  $\gamma p \rightarrow \pi^0 p$ . The multipoles corresponding to the  $S$ - and  $P$ -wave approximation discussed here are

$$\{E_{0+}, E_{1+}, M_{1+}, M_{1-}\}. \quad (75)$$

For the starting MAID solution, the real and imaginary parts are plotted in Fig. 1. The task now consists of finding all possible sets of additional solutions that leave the group  $S$  observables invariant and that are consistent with the underlying formalism, i.e., fulfill the consistency relation (40). The procedure starts with the MAID solution. For  $L = \ell_{\text{max}} = 1$ , i.e.,  $S$  and  $P$  waves, the normalized polynomials  $A_{2L}(t)$  and  $B_{2L}(t)$  from Eqs. (30) and (31) become, with  $t = \tan \theta/2$ ,

$$\begin{aligned} A_2(t) &= t^2 + \hat{a}_1 t + \hat{a}_0 \\ &= t^2 + 2i \frac{2M_{1+} + M_{1-}}{E_{0+} - 3E_{1+} - M_{1+} + M_{1-}} t \\ &\quad + \frac{E_{0+} + 3E_{1+} + M_{1+} - M_{1-}}{E_{0+} - 3E_{1+} - M_{1+} + M_{1-}}, \end{aligned} \quad (76)$$

$$\begin{aligned} B_2(t) &= t^2 + \hat{b}_1 t + \hat{b}_0 \\ &= t^2 + 2i \frac{3E_{1+} - M_{1+} + M_{1-}}{E_{0+} - 3E_{1+} - M_{1+} + M_{1-}} t \\ &\quad + \frac{E_{0+} + 3E_{1+} + M_{1+} - M_{1-}}{E_{0+} - 3E_{1+} - M_{1+} + M_{1-}}. \end{aligned} \quad (77)$$

For this case the normalization coefficient is  $a_2 = b_2 = E_{0+} - 3E_{1+} - M_{1+} + M_{1-}$ . The modulus of the normalization factor, or coefficient  $a_2$ , is given by

$$|a_2|^2 = I(\pi). \quad (78)$$

Therefore, as mentioned in Sec. III, in this reformulation using polynomials,  $a_2$  carries the undeterminable overall phase of the multipoles. Once all coefficients, i.e.,  $a_2$ ,  $\hat{a}_1$ ,  $\hat{a}_0$ ,  $\hat{b}_1$ , and  $\hat{b}_0$  are evaluated for each energy bin using the solution MAID2007, the next step is to find the roots  $\{\alpha_1, \alpha_2\}$  for the polynomial (76) and  $\{\beta_1, \beta_2\}$  for Eq. (77). This task, as well as every other numerical calculation mentioned in this section, was performed using the computer algebra tool MATHEMATICA. The polynomials  $A_2$  and  $B_2$  in this case acquire the linear factor decomposition

$$\begin{aligned} A_2(t) &= (t - \alpha_1)(t - \alpha_2), \\ B_2(t) &= (t - \beta_1)(t - \beta_2). \end{aligned} \quad (79)$$

With the obtained roots it is easy to check that the consistency relation (40) for the case  $L = 1$  reads

$$\alpha_1 \alpha_2 = \beta_1 \beta_2, \quad (80)$$

which is fulfilled for every energy bin by the starting MAID solution. As mentioned in Sec. III, all candidates for ambiguous solutions are constructed by complex conjugation of roots. However, the argument in this section shall be made in an equivalent way by using the phases of the roots [25]. For the latter, the consistency relation, defining  $\alpha_k = |\alpha_k| e^{i\varphi_k}$  and  $\beta_l = |\beta_l| e^{i\psi_l}$ , reads

$$\varphi_1 + \varphi_2 = \psi_1 + \psi_2. \quad (81)$$

The search for ambiguous solutions now consists of checking which different choices of the signs in Eq. (81) also yield a valid equality. The arising possibilities can, for the case  $L = 1$ , be summarized by means of the equation

$$\pm \varphi_1 \pm \varphi_2 = \pm \psi_1 \pm \psi_2. \quad (82)$$



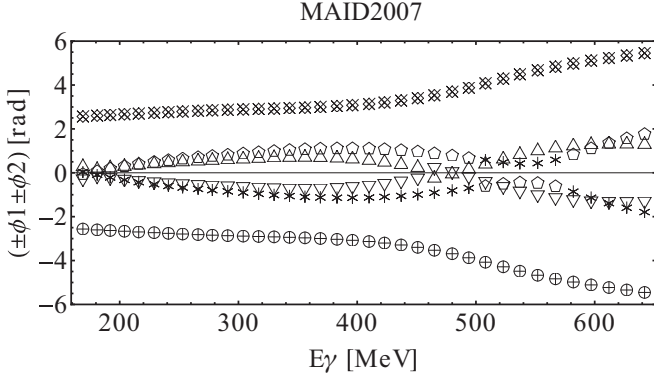


FIG. 2. Ambiguity diagram for the  $S$ - and  $P$ -wave multipoles (i.e.,  $L = \ell_{\max} = 1$ ) of the MAID2007 solution as explained in the text. Plotted are different sign choices for linear combinations of phases  $\{\varphi_1, \varphi_2\}$  and  $\{\psi_1, \psi_2\}$ , respectively. The scheme of labeling the different linear combinations is the following:  $\circ$  ( $\varphi_1 + \varphi_2$ ),  $\triangle$  ( $\varphi_1 - \varphi_2$ ),  $\nabla$  ( $-\varphi_1 + \varphi_2$ ),  $\diamond$  ( $-\varphi_1 - \varphi_2$ ),  $+$  ( $\psi_1 + \psi_2$ ),  $*$  ( $\psi_1 - \psi_2$ ),  $\diamond$  ( $-\psi_1 + \psi_2$ ),  $\times$  ( $-\psi_1 - \psi_2$ ).

Before the above-mentioned procedure is described further, it is worth mentioning the way in which one can calculate the corresponding multipoles, once new sets of phases and therefore also roots are obtained. Phases and roots can yield the polynomial coefficients. All that has to be done is to fully expand the linear factorization (79). The result, relating roots and normalized polynomial coefficients, reads

$$\hat{a}_1 = -\alpha_1 - \alpha_2, \quad \hat{a}_0 = \alpha_1 \alpha_2, \quad (83)$$

$$\hat{b}_1 = -\beta_1 - \beta_2, \quad \hat{b}_0 = \beta_1 \beta_2. \quad (84)$$

For the connection between coefficients and multipoles there exist linear relations, as can be anticipated by inspection of Eqs. (76) and (77). For the case  $L = 1$  the following identities hold:

$$E_{0+} = \frac{1}{2} a_2 (1 + \hat{a}_0), \quad (85)$$

$$E_{1+} = \frac{1}{12} a_2 (\hat{a}_0 - 1 - i \hat{b}_1), \quad (86)$$

$$M_{1+} = \frac{1}{12} a_2 (\hat{a}_0 - 1 - 2i \hat{a}_1 + i \hat{b}_1), \quad (87)$$

$$M_{1-} = \frac{1}{6} a_2 (1 - \hat{a}_0 - i \hat{a}_1 - i \hat{b}_1). \quad (88)$$

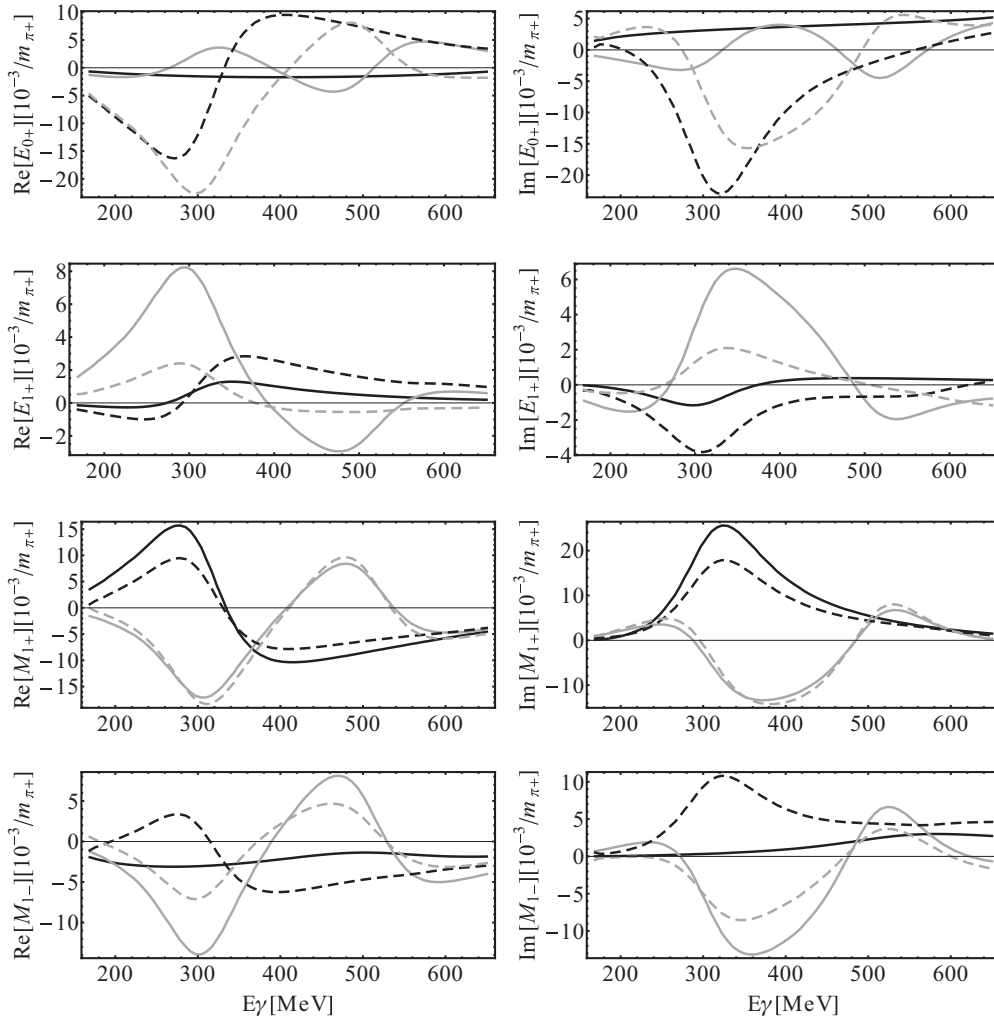


FIG. 3.  $S$ - and  $P$ -wave multipole ambiguities of the group  $S$  observables extracted from Fig. 2. The starting solution is given by the solid black curves, the double ambiguity by the solid gray curves. The accidental ambiguities owing to Eqs. (90) and (91) are plotted as dashed black and dashed gray curves, respectively.

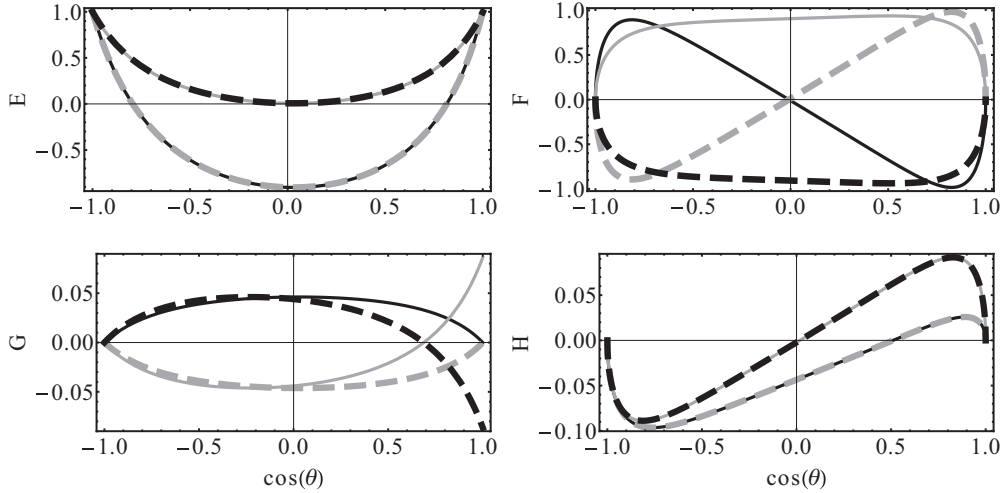


FIG. 4. Results of BT observables using the four different solutions deduced from Fig. 2. Therefore, only  $S$ - and  $P$ -wave multipoles contribute. The starting solution is given by the solid black curves, the double ambiguity by the thick dashed gray curves. The accidental ambiguities (90) and (91) are represented by the solid gray and thick dashed black curves, respectively. For the observables  $F$  and  $G$ , all solutions are discriminable, which is not true for  $E$  and  $H$ . All observables are plotted versus the angular variable  $\cos\theta$ . The energy bin of  $E_{\gamma}^{\text{LAB}} = 253$  MeV was chosen for this picture.

For  $L = 2$ , Appendix B contains the corresponding relations as a more extensive example. However, relations similar in structure to the examples in this section can be derived for every finite order in  $L$ . Because roots and multipoles are now established as fully equivalent sets of complex variables, the description of the numerical ambiguity study is continued. For each energy bin and for each combination of phases appearing in Eq. (82), the consistency relation has to be checked separately. The result of this procedure can be summarized by a plot that from now on is referred to as the ambiguity diagram, given in Fig. 2 (this type of diagram is also given in Ref. [25]). In this plot every possible case of sign choices in the linear combinations of the phases  $\{\varphi_1, \varphi_2\}$  and  $\{\psi_1, \psi_2\}$  is drawn versus photon laboratory energy  $E_{\gamma}^{\text{LAB}}$ . The caption of Fig. 2 provides the legend for the symbols used in the ambiguity diagrams. Once a symbol representing the left-hand side of Eq. (82) coincides with one representing the right-hand side, the consistency relation is fulfilled and an ambiguity of the group S observables has to be expected. For the starting solution this criterion is naturally fulfilled for every energy bin, as depicted by the symbols  $\circ$  and  $+$  in Fig. 2 [see Eq. (81)]. Once all roots are conjugated simultaneously, i.e.,

$$\alpha \rightarrow \alpha^*, \quad \beta \rightarrow \beta^*, \quad (89)$$

the predicted double ambiguity is obtained (see Sec. III). It corresponds to the symbols  $\diamond$  and  $\times$  in Fig. 2. In addition to the predictable ambiguities, numerically accidental ambiguities are also possible. The remaining sign choices  $(+, -)$  and  $(-, +)$  are also given by their corresponding symbols in Fig. 2. As can be observed, symbols in these two cases exactly coincide only for three cases at roughly 220, 515, and 615 MeV. Looking at the remaining energy bins, however, it can be observed that the symbols are getting quite close. Therefore, two additional

ambiguous solutions can be expected for the cases

$$\varphi_1 - \varphi_2 \approx -\psi_1 + \psi_2, \quad (90)$$

as well as

$$-\varphi_1 + \varphi_2 \approx \psi_1 - \psi_2. \quad (91)$$

Using Eqs. (83) to (88), the predicted as well as the accidental ambiguities deduced from Fig. 2 can be translated into multipoles. The results are shown and explained in Fig. 3. As can be observed, all solutions are smooth and distinct from each other. Therefore, in case of a model-independent TPWA, the expectation is that for an  $S$ - and  $P$ -wave truncation the group S observables will not be able to distinguish among the four solutions plotted in Fig. 3. Once Eqs. (54) to (57) are used to calculate group S observables, it can be seen that the results for the four different solutions exactly coincide (this can also be seen from the formalism of Sec. III). The ingredient that is needed to decide which of the four solution candidates is the correct one are double polarization observables. Because the observables of the class BT are the most experimentally accessible ones, the focus is drawn to them. Figure 4 shows plots that result from the application of Eqs. (63) to (66) to the four ambiguous solutions deduced in this study. The BT observables are calculated and drawn such that they can be graphically distinguished from each other. The energy bin  $E_{\gamma}^{\text{LAB}} = 253$  MeV was chosen as an example. As can be observed, for the observables  $E$  and  $H$ , the starting solution and the double ambiguity as well as both accidental ambiguities exactly coincide. Therefore, it is expected that in a TPWA, data for both observables will not be able to distinguish among the corresponding ambiguities, in particular, not between the double ambiguity and the starting solution.  $F$  and  $G$ , however, show differing curves for all four solutions, which means that both observables should be capable of yielding the correct unique solution

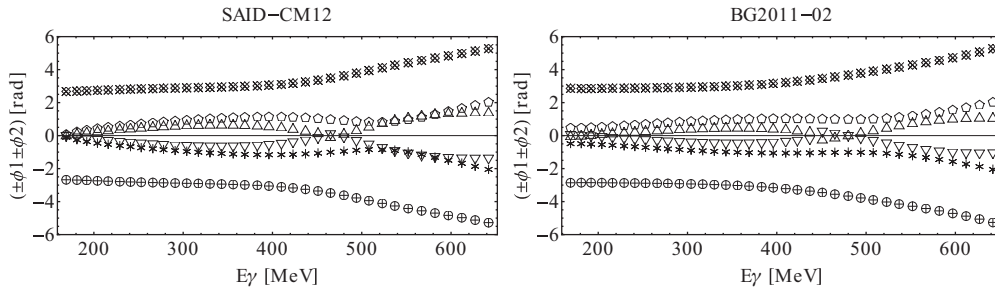


FIG. 5. Ambiguity diagrams for the  $S$ - and  $P$ -wave multipoles of different PWAs. The left and right panels are obtained by using the CM12 solution of the SAID group and the BG2011-02 solution of the Bonn-Gatchina group, respectively. The symbols chosen are as in Fig. 2.

in the performed fit. Another feature that can be observed for the observable  $G$  is that both solutions corresponding to the accidental ambiguities postulated in this section show a behavior that contradicts the rules deduced in Sec. IV, i.e.,  $G$  does not approach 0 for  $\cos\theta \rightarrow 1$ . Inspecting the ambiguity diagram for  $E_\gamma^{\text{LAB}} = 253$  MeV, the phases are close but do not completely overlap and the consistency relation is not exactly fulfilled. With high-precision data this can be distinguished; for data with sizable errors it could well show up as an additional ambiguity.

As a result of the ambiguity study presented until now, it should be stated that in the context of a TPWA with  $L = 1$ , i.e.,  $S$  and  $P$  waves, the following minimum subsets of observables already form complete sets that exclude the need for experimental information on recoil polarization:

$$\{\sigma_0, \Sigma, T, P, F\}, \quad \{\sigma_0, \Sigma, T, P, G\}. \quad (92)$$

The numerical input for the ambiguity study performed in this work consists of a solution for multipoles given by the MAID PWA [27]. Because it is well known that the current state-of-the-art PWAs show quite some deviations [35] already for  $S$ - and  $P$ -wave multipoles, it is interesting to compare the ambiguity diagrams for different solutions. Figure 5 shows the diagrams obtained from multipoles of the SAID group [28] as well as of the Bonn-Gatchina group [29].

For all three PWAs, the diagrams show a similar structure. Symbols referring to the starting solution as well as the double ambiguity in each case inhabit the same areas in the plot. The most visible differences are seen in the closeness of the symbols defining the possible accidental ambiguities at lower energies as well as the possible appearance of intersections for higher energies. At low energies, symbols are most nearby for the MAID2007 solution, for which the corresponding ambiguities have already been ruled out. Therefore, it is expected that any possible accidental ambiguities are also negligible at low energies for the SAID and BnGa solutions. This comparison of different PWAs concludes the discussion on the  $S$ - and  $P$ -wave truncation in this section.

## VI. CONCLUSION AND OUTLOOK

This work contains a treatment of the ambiguity problem that arises in the TPWA of pseudoscalar meson photoproduction in a consideration of single channels that have highly suppressed  $t$ -channel exchanges. For this purpose,

the approach of Omelaenko from 1981 [25] was revisited and supplemented by more information on intermediate calculational steps. This above-mentioned approach consists of first searching for all possible ambiguities of the group  $S$  observables and then selecting appropriate double polarization measurements that can remove all additional solutions. One ambiguity, called the double ambiguity, can be predicted just by the formalism. It can be removed for all energy regions and all orders in the truncation angular momentum  $L$  by a measurement of the observables  $G$  and  $F$  or any BR as well as TR double polarization observable. However, there can also exist numerically accidental ambiguities that may require information on additional double polarization observables.

As a numerical application of the presented formalism, the investigation of an  $S$ - and  $P$ -wave truncation (i.e.,  $L = 1$ ) also executed similarly in Ref. [25] was done using multipoles of the PWA solution MAID2007 [27] as input. It was found that for this situation, i.e., in a treatment that disregards measurement uncertainty, accidental ambiguities can be neglected and only the double ambiguity has to be removed. Therefore, in this case the sets of five observables

$$\{\sigma_0, \Sigma, T, P, F\}, \quad \{\sigma_0, \Sigma, T, P, G\},$$

can be postulated as complete sets of observables for this simplest case in the context of the study. As derived in Sec. IV, the double polarization observables  $F$  or  $G$  can also be replaced by any one of the recoil observables of the groups BR and TR.

The development of the situation for increasing  $L$  is as follows. The number of new sets of potentially ambiguous solutions is  $2^{4L}$  for every  $L$ . Although not all of these solutions have to fulfill all of the consistency requirements to be regarded as realistic ambiguities, the number of candidates that potentially could fulfill all those requirements is vastly increasing. This increasing difficulty with growing angular momentum  $L$  is also described in Ref. [25]. It is therefore likely that, at least as soon as real data are fitted, the complete sets given above have to be extended by additional observables for higher values of  $L$ .

As an outlook it is interesting whether the results found in this work apply to the numerical fitting of data. The following procedure is proposed for these fits. First, numerical precision data for polarization observables generated by use of existing PWA solutions should be fitted. These data do not carry statistical fluctuations and have numerical uncertainties given

by the number of digits in the tables. In this case it is expected that the accidental ambiguities are not significant, because only precise equalities of phases are relevant, which are relatively infrequent. The numerical precision data could then be used to generate pseudodata that are closer to the realistic situation by carrying adjustable uncertainties [17]. Fits to these data then have to show how significant the impact of varying uncertainties is on the appearance of additional ambiguous solutions. However, both fitting procedures proposed until now are only preparatory steps. The final goal is to investigate the fitting to real data from the world database of a specific photoproduction channel, for example,  $\gamma p \rightarrow \pi^0 p$ .

It remains to be seen whether it will be possible to arrive at a final unique multipole solution by using only group S and BT double polarization observables, exclusively.

### ACKNOWLEDGMENTS

This work was supported by the Deutsche Forschungsgemeinschaft (Grants No. SFB/TR16 and No. SFB 1044) and the European Community-Research Infrastructure Activity (Grant No. FP7). The authors would like to thank all members of the Bonn-Gatchina group for fruitful discussions and Annika Thiel for the careful reading of the manuscript.

### APPENDIX A: DERIVATION OF EXPLICIT EXPRESSIONS FOR ANGULAR POLYNOMIALS

The multipole expansion of Eqs. (4) to (7) can be written in a more convenient form for a truncation at finite  $L$ ,

$$F_1(W, \theta) = \sum_{\ell=0}^L \{f_\ell^{(1)}(W)P'_{\ell+1}(x) + f_\ell^{(2)}(W)P'_{\ell-1}(x)\}, \quad (\text{A1})$$

$$F_2(W, \theta) = \sum_{\ell=1}^L f_\ell^{(3)}(W)P'_\ell(x), \quad (\text{A2})$$

$$F_3(W, \theta) = \sum_{\ell=1}^L \{f_\ell^{(4)}(W)P''_{\ell+1}(x) + f_\ell^{(5)}(W)P''_{\ell-1}(x)\}, \quad (\text{A3})$$

$$F_4(W, \theta) = \sum_{\ell=2}^L f_\ell^{(6)}(W)P''_\ell(x), \quad (\text{A4})$$

with  $x = \cos \theta$  and the following six energy-dependent functions:

$$f_\ell^{(1)}(W) = \ell M_{\ell+}(W) + E_{\ell+}(W), \quad (\text{A5})$$

$$f_\ell^{(2)}(W) = (\ell + 1)M_{\ell-}(W) + E_{\ell-}(W), \quad (\text{A6})$$

$$f_\ell^{(3)}(W) = (\ell + 1)M_{\ell+}(W) + \ell M_{\ell-}(W), \quad (\text{A7})$$

$$f_\ell^{(4)}(W) = E_{\ell+}(W) - M_{\ell+}(W), \quad (\text{A8})$$

$$f_\ell^{(5)}(W) = E_{\ell-}(W) + M_{\ell-}(W), \quad (\text{A9})$$

$$f_\ell^{(6)}(W) = M_{\ell+}(W) - E_{\ell+}(W) - M_{\ell-}(W) - E_{\ell-}(W). \quad (\text{A10})$$

It is useful to introduce the Pochhammer symbols [30],

$$(a)_m := a(a+1)\cdots(a+m-1), \quad (a)_0 := 1. \quad (\text{A11})$$

For the special cases  $(a)_1$  and  $(1)_m$  this definition yields

$$(a)_1 = a, \quad (1)_m = m!. \quad (\text{A12})$$

The symbols  $(a)_m$  appear in the expansion of the hypergeometric function [30,36],

$${}_2F_1(a, b; c; Z) := \sum_{m=0}^{\infty} \frac{(a)_m (b)_m}{(c)_m m!} Z^m, \quad (\text{A13})$$

for real quantities  $a, b, c$  and a generally complex argument  $Z \in \mathbb{C}$ . Equation (A13) corresponds to a particular choice of indices in the definition of the generalized hypergeometric function,

$${}_nF_m(a_1, \dots, a_n; b_1, \dots, b_m; Z) := \sum_{k=0}^{\infty} \frac{(a_1)_k \cdots (a_n)_k}{(b_1)_k \cdots (b_m)_k k!} Z^k. \quad (\text{A14})$$

It is important to note that the Legendre polynomials  $P_\ell(\cos \theta)$  can be expressed in terms of hypergeometric functions (i.e., Ref. [30]),

$$P_\ell(\cos \theta) = {}_2F_1\left(-\ell, \ell + 1; 1; \frac{1-c}{2}\right), \quad (\text{A15})$$

where on the right-hand side the abbreviation  $c = \cos \theta$  was chosen in the argument of  ${}_2F_1$ . This work features an exchange of the angular variable  $c = \cos \theta$  for  $t = \tan \theta/2$ . Equation (A15), with the right-hand side rewritten in terms of  $t$ , takes the form [30]

$$P_\ell(\cos \theta) = (1+t^2)^{-\ell} {}_2F_1(-\ell, -\ell; 1; -t^2). \quad (\text{A16})$$

The idea is to rewrite all derivatives of Legendre polynomials appearing in Eqs. (A1) to (A4) in terms of hypergeometric functions  ${}_2F_1$  depending on  $t$ . To do this, a relation is needed that can be inferred from Eq. (15.2.7) of Ref. [36]

$$\begin{aligned} \frac{d}{dZ}[(1-Z)^a {}_2F_1(a, b; c; Z)] \\ = (-) \frac{a(c-b)}{c} (1-Z)^{a-1} \times {}_2F_1(a+1, b; c+1; Z). \end{aligned} \quad (\text{A17})$$

This identity is necessary for the determination of the derivative of  $P_\ell(\cos \theta)$ . The first-order derivative  $P'_\ell(\cos \theta)$  can be rearranged as

$$\begin{aligned} P'_\ell(\cos \theta) &= \frac{d}{d \cos \theta} P_\ell(\cos \theta) \\ &= \frac{d}{d \cos \theta} [(1+t^2)^{-\ell} {}_2F_1(-\ell, -\ell; 1; -t^2)] \\ &= \frac{d}{dt^2} [(1+t^2)^{-\ell} {}_2F_1(-\ell, -\ell; 1; -t^2)] \times \frac{dt^2}{d \cos \theta}. \end{aligned} \quad (\text{A18})$$

Inspection of Eq. (16) facilitates the evaluation of the second factor in the relation given above, i.e.,

$$\begin{aligned} \frac{dt^2}{d \cos \theta} &= \frac{d}{d \cos \theta} \tan^2 \frac{\theta}{2} = \frac{d}{d \cos \theta} \left[ \frac{1 - \cos \theta}{1 + \cos \theta} \right] \\ &= -\frac{2}{(1 + \cos \theta)^2} = -\frac{1}{2}(1 + t^2)^2. \end{aligned} \quad (\text{A19})$$

The identity (A17) yields the first factor on the right-hand side of Eq. (A18), so that the final result becomes

$$P'_\ell(\cos \theta) = \frac{1}{2} \ell(\ell + 1)(1 + t^2)^{-\ell+1} {}_2F_1(-\ell + 1, -\ell; 2; -t^2). \quad (\text{A20})$$

The same procedure also yields an expression for the second derivative of  $P_\ell(\cos \theta)$

$$\begin{aligned} P''_\ell(\cos \theta) &= \frac{1}{8}(\ell - 1)\ell(\ell + 1)(\ell + 2)(1 + t^2)^{-\ell+2} \\ &\quad \times {}_2F_1(-\ell + 2, -\ell; 3; -t^2). \end{aligned} \quad (\text{A21})$$

Everything assembled until now facilitates the evaluation of the polynomial  $A'_{2L}(t)$  that appears in the amplitude  $b_4$  of Eq. (17). First of all, the term  $[F_1(\theta) - (\cos \theta - i \sin \theta)F_2(\theta)]$  that can be deduced from Eq. (11), when written in terms of the variable  $t$  reads [see Eq. (15)]

$$\left[ F_1(\theta) + \frac{1}{(1 + t^2)}(t + i)^2 F_2(\theta) \right]. \quad (\text{A22})$$

Insertion of the multipole expansions (A1) and (A2) yields

$$\begin{aligned} \sum_{\ell=0}^L \left[ f_\ell^{(1)} P'_{\ell+1}(\cos \theta) + f_\ell^{(2)} P'_{\ell-1}(\cos \theta) \right. \\ \left. + \frac{(t + i)^2}{(1 + t^2)} f_\ell^{(3)} P'_\ell(\cos \theta) \right]. \end{aligned} \quad (\text{A23})$$

Usage of (A20) and pulling out an overall factor  $(1 + t^2)^{-L}$  out of the sum already gives the result for  $b_4$  given in the main text

$$\begin{aligned} b_4(\theta) &= \frac{C \exp[i\theta/2]}{4(1 + t^2)^L} \sum_{\ell=0}^L \left\{ f_\ell^{(1)}(\ell + 1)(\ell + 2)(1 + t^2)^{L-\ell} {}_2F_1(-\ell, -\ell - 1; 2; -t^2) \right. \\ &\quad + f_\ell^{(2)}\ell(\ell - 1)(1 + t^2)^{L-\ell+2} {}_2F_1(-\ell + 2, -\ell + 1; 2; -t^2) \\ &\quad \left. + f_\ell^{(3)}\ell(\ell + 1)(t + i)^2(1 + t^2)^{L-\ell} {}_2F_1(-\ell + 1, -\ell; 2; -t^2) \right\}. \end{aligned} \quad (\text{A24})$$

To determine the polynomial  $B'_{2L}(t) = A'_{2L}(t) + tD'_{2L-2}(t)$  of the amplitude  $b_2$  of Eq. (18), it is sufficient to infer the form of  $D'_{2L-2}(t)$  by inspection of the formula (9). It is therefore necessary to rewrite the term

$$i \sin \theta [F_3(\theta) + (\cos \theta - i \sin \theta)F_4(\theta)] \quad (\text{A25})$$

in terms of the variable  $t$ ,

$$\frac{2it}{(1 + t^2)} \left[ F_3(\theta) - \frac{1}{(1 + t^2)}(t + i)^2 F_4(\theta) \right]. \quad (\text{A26})$$

Invoking the multipole expansions (A3) and (A4) yields

$$\frac{2it}{(1 + t^2)} \sum_{\ell=0}^L \left[ f_\ell^{(4)} P''_{\ell+1}(\cos \theta) + f_\ell^{(5)} P''_{\ell-1}(\cos \theta) - \frac{(t + i)^2}{(1 + t^2)} f_\ell^{(6)} P''_\ell(\cos \theta) \right]. \quad (\text{A27})$$

Usage of (A21) in a similar way yields the expression for  $D'_{2L-2}(t)$  that is already given in Eq. (18) of the main text,

$$\begin{aligned} D'_{2L-2}(t) &= \frac{1}{4} \sum_{\ell=0}^L \left\{ (i f_\ell^{(4)})\ell(\ell + 1)(\ell + 2)(\ell + 3)(1 + t^2)^{L-\ell} {}_2F_1(-\ell + 1, -\ell - 1; 3; -t^2) \right. \\ &\quad + (i f_\ell^{(5)})(\ell - 2)(\ell - 1)\ell(\ell + 1)(1 + t^2)^{L-\ell+2} {}_2F_1(-\ell + 3, -\ell + 1; 3; -t^2) \\ &\quad \left. - (i f_\ell^{(6)})(\ell - 1)\ell(\ell + 1)(\ell + 2)(t + i)^2(1 + t^2)^{L-\ell} {}_2F_1(-\ell + 2, -\ell; 3; -t^2) \right\}. \end{aligned} \quad (\text{A28})$$

Furthermore, the expressions for  $A'_{2L}(t)$  and  $B'_{2L}(t)$  given in this appendix can be further simplified and be brought into the form

$$A'_{2L}(t) = \sum_{\ell=0}^{2L} a_\ell t^\ell, \quad (\text{A29})$$

$$B'_{2L}(t) = \sum_{\ell=0}^{2L} b_\ell t^\ell, \quad (\text{A30})$$

with explicit formulas for the complex expansion coefficients  $a_\ell$  and  $b_\ell$  in terms of multipoles (see Ref. [30], where similar expressions are given for  $\pi N$  scattering).

APPENDIX B: LINEAR RELATIONS AMONG  $\{a_i, b_i\}$  AND  $\{E_{\ell\pm}, M_{\ell\pm}\}$  FOR  $L = 1$  AND  $L = 2$ 

Following are linear relations among multipoles and complex polynomial coefficients for  $L = 1$ :

$$\begin{bmatrix} E_{0+} \\ E_{1+} \\ M_{1+} \\ M_{1-} \end{bmatrix} = \frac{a_2}{2} \begin{bmatrix} 1 & 1 & 0 & 0 \\ -\frac{1}{6} & \frac{1}{6} & 0 & -\frac{i}{6} \\ -\frac{1}{6} & \frac{1}{6} & -\frac{i}{3} & \frac{i}{6} \\ \frac{1}{3} & -\frac{1}{3} & -\frac{i}{3} & -\frac{i}{3} \end{bmatrix} \begin{bmatrix} 1 \\ \hat{a}_0 \\ \hat{a}_1 \\ \hat{b}_1 \end{bmatrix}. \quad (\text{B1})$$

Similar relations for the case  $L = 2$  are as follows:

$$\begin{bmatrix} E_{0+} \\ E_{1+} \\ M_{1+} \\ M_{1-} \\ E_{2+} \\ E_{2-} \\ M_{2+} \\ M_{2-} \end{bmatrix} = \frac{a_4}{2} \begin{bmatrix} \frac{2}{3} & \frac{2}{3} & 0 & \frac{1}{6} & 0 & 0 & \frac{1}{6} & 0 \\ -\frac{1}{6} & \frac{1}{6} & 0 & 0 & 0 & -\frac{i}{12} & 0 & -\frac{i}{12} \\ -\frac{1}{6} & \frac{1}{6} & -\frac{i}{6} & 0 & -\frac{i}{6} & \frac{i}{12} & 0 & \frac{i}{12} \\ \frac{1}{3} & -\frac{1}{3} & -\frac{i}{6} & 0 & -\frac{i}{6} & -\frac{i}{6} & 0 & -\frac{i}{6} \\ \frac{1}{45} & \frac{1}{45} & 0 & 0 & 0 & -\frac{i}{45} & -\frac{1}{45} & \frac{i}{45} \\ \frac{1}{30} & \frac{1}{30} & 0 & \frac{1}{12} & 0 & \frac{i}{20} & -\frac{7}{60} & -\frac{i}{20} \\ \frac{1}{45} & \frac{1}{45} & -\frac{i}{30} & -\frac{1}{30} & \frac{i}{30} & \frac{i}{90} & \frac{1}{90} & -\frac{i}{90} \\ -\frac{1}{30} & -\frac{1}{30} & -\frac{i}{30} & \frac{1}{20} & \frac{i}{30} & -\frac{i}{60} & -\frac{1}{60} & \frac{i}{60} \end{bmatrix} \begin{bmatrix} 1 \\ \hat{a}_0 \\ \hat{a}_1 \\ \hat{a}_2 \\ \hat{a}_3 \\ \hat{b}_1 \\ \hat{b}_2 \\ \hat{b}_3 \end{bmatrix}. \quad (\text{B2})$$

- [1] J. Beringer *et al.* (Particle Data Group Collaboration), *Phys. Rev. D* **86**, 010001 (2012).
- [2] A. V. Anisovich, R. Beck, E. Klempt, V. A. Nikonov, A. V. Sarantsev, and U. Thoma, *Eur. Phys. J. A* **48**, 15 (2012).
- [3] G. Hoehler, *Pion Nucleon Scattering, Part 2, Landolt-Bornstein: Elastic and Charge Exchange Scattering of Elementary Particles* (Springer-Verlag, Berlin, 1983), Vol. 9b.
- [4] R. E. Cutkosky, C. P. Forsyth, R. E. Hendrick, and R. L. Kelly, *Phys. Rev. D* **20**, 2839 (1979).
- [5] R. A. Arndt, W. J. Briscoe, I. I. Strakovsky, and R. L. Workman, *Phys. Rev. C* **74**, 045205 (2006).
- [6] D. Drechsel, S. S. Kamalov, and L. Tiator, *Eur. Phys. J. A* **34**, 69 (2007).
- [7] G. Y. Chen, S. S. Kamalov, S. N. Yang, D. Drechsel, and L. Tiator, *Phys. Rev. C* **76**, 035206 (2007).
- [8] D. Roenchen, M. Doring, F. Huang, H. Haberzettl, J. Haidenbauer, C. Hanhart, S. Krewald, U.-G. Meissner *et al.*, *Eur. Phys. J. A* **49**, 44 (2013).
- [9] H. Kamano, S. X. Nakamano, T.-S. H. Lee, and T. Sato, *Phys. Rev. C* **88**, 035209 (2013).
- [10] M. Shrestha and D. M. Manley, *Phys. Rev. C* **86**, 055203 (2012).
- [11] V. Shklyar, H. Lenske, and U. Mosel, *Phys. Rev. C* **87**, 015201 (2013).
- [12] G. F. Chew, M. L. Goldberger, F. E. Low, and Y. Nambu, *Phys. Rev.* **106**, 1345 (1957).
- [13] I. S. Barker, A. Donnachie, and J. K. Storrow, *Nucl. Phys. B* **95**, 347 (1975).
- [14] G. Keaton and R. Workman, *Phys. Rev. C* **54**, 1437 (1996).
- [15] W.-T. Chiang and F. Tabakin, *Phys. Rev. C* **55**, 2054 (1997).
- [16] D. G. Ireland, *Phys. Rev. C* **82**, 025204 (2010).
- [17] R. L. Workman, M. W. Paris, W. J. Briscoe, L. Tiator, S. Schumann, M. Ostrick, and S. S. Kamalov, *Eur. Phys. J. A* **47**, 143 (2011).
- [18] A. M. Sandorfi, S. Hoblit, H. Kamano, and T.-S. H. Lee, *J. Phys. G* **38**, 053001 (2011).
- [19] T. Vranckx, J. Ryckebusch, T. Van Cuyck, and P. Vancraeyveld, *Phys. Rev. C* **87**, 055205 (2013).
- [20] M. H. Sikora, D. P. Watts, D. I. Glazier, P. Aguar-Bartolome, L. K. Akasoy, J. R. M. Annand, H. J. Arends, K. Bantawa *et al.*, *Phys. Rev. Lett.* **112**, 022501 (2014).
- [21] M. L. Goldberger, H. W. Lewis, and K. M. Watson, *Phys. Rev.* **132**, 2764 (1963).
- [22] I. P. Ivanov, *Phys. Rev. D* **85**, 076001 (2012).
- [23] L. Tiator, *AIP Conf. Proc.* **1432**, 162 (2012).
- [24] L. Tiator, *Proceedings of the Bled Workshops in Physics*, Vol. 13, No. 1 (J. Stefan Institute, University of Ljubljana, Ljubljana, Slovenia, 2012), p. 55.
- [25] A. S. Omelaenko, *Sov. J. Nucl. Phys.* **34**, 406 (1981).
- [26] V. F. Grushin, in *Photoproduction of Pions on Nucleons and Nuclei*, edited by A. A. Komar (Nova Science, New York, 1989), p. 1ff.
- [27] MAID Partial Wave Analysis, <http://www.kph.uni-mainz.de/MAID/>
- [28] SAID Partial Wave Analysis, <http://gwdac.phys.gwu.edu/>
- [29] Bonn Gatchina Partial Wave Analysis, <http://pwa.hiskp.uni-bonn.de/>
- [30] A. Gersten, *Nucl. Phys. B* **12**, 537 (1969).
- [31] E. Barrelet, *Nuovo Cimento* **8A**, 331 (1972).
- [32] A. J. Van Horn, *Nucl. Phys. B* **87**, 157 (1975).
- [33] C. G. Fasano, F. Tabakin, and B. Saghai, *Phys. Rev. C* **46**, 2430 (1992).
- [34] A. M. Sandorfi, B. Dey, A. Sarantsev, L. Tiator, and R. Workman, *AIP Conf. Proc.* **1432**, 219 (2012).
- [35] A. V. Anisovich, E. Klempt, V. A. Nikonov *et al.*, *Eur. Phys. J. A* **44**, 203 (2010).
- [36] M. Abramowitz and I. A. Stegun, *Handbook of Mathematical Functions* (Dover, Mineola, NY, 1972).